A Novel Missense Mutation Shows that GPIbβ Has a Dual Role in Controlling the Processing and Stability of the Platelet GPIb-IX Adhesion Receptor

Catherine Strassel,[‡] Jean-Max Pasquet,[§] Marie-Christine Alessi,[‡,||] Irène Juhan-Vague,[‡,||] Hervé Chambost,[‡,||] Robert Combrié,[§] Paquita Nurden,[§] Marie-Jeanne Bas,[‡] Corinne De La Salle,[‡] Jean-Pierre Cazenave,[‡] François Lanza,[‡] and Alan T. Nurden*[,§]

INSERM U311-Etablissement Français du Sang, 10 rue Spielmann/BP 36, Strasbourg Cedex, Laboratoire d'Hématologie, CHU Timone, Marseille Cedex, and UMR 5533 CNRS, Hôpital Cardiologique, 33604 Pessac, France

Received May 29, 2002; Revised Manuscript Received October 23, 2002

ABSTRACT: Glycoprotein (GP) Ibα is a major adhesive receptor of platelets, surface expressed as part of the GPIb-IX-V complex. However, important questions about how the four gene products (Ibα, Ibβ, IX, and V) composing this complex are processed remain. A deficiency of or nonfunctioning GPIb-IX-V is characteristic of the Bernard-Soulier syndrome (BSS), an inherited bleeding disease. We now report a BSS variant whose platelets have little or no GIbβ or GPIX, but where residual GPIbα was selectively located in flow cytometry by monoclonal antibodies (WM23 and Bx-1) recognizing denatured epitopes. Whereas WM23 immunoprecipitated GPIbα (130 kDa), GPIX, and GPIbβ from control platelets, a single surface protein of $\approx$66 kDa was obtained for the patient. DNA sequencing revealed a homozygous Asn^{64} → Thr substitution in the GPIbβ from the patient. This substitution modified a conserved residue in the COOH-terminal region flanking the single-copy leucine-rich domain of GPIbβ. When GPIbβ64Thr was coexpressed in a stable CHO cell line with wild-type GPIbα and GPIX, flow cytometry and confocal microscopy failed to show GPIb-IX complexes at the cell surface. Intracellular GPIbα and GPIbβ were detected and largely confined to the endoplasmic reticulum, and little GPIX was seen. GPIbα was immunoprecipitated as a 66−70 kDa protein in ^{35}S metabolic studies and lacked O-glycosidic side chains. Also, it was not disulfide bound to the mutated GPIbβ. Thus, a single amino acid substitution in the extracellular domain of GPIbβ can affect both the maturation of GPIbα and GPIX stability. GPIbβ has a pivotal role in regulating GPIb-IX-V biosynthesis.

Platelet interaction with von Willebrand factor (vWF)[1] during thrombus formation first involves collagen-bound vWF exposed at sites of blood vessel injury (*1*). This process depends on an initial interaction with the GPIb-IX-V complex and the subsequent stabilization of the adherence after activation of integrins $\alpha 2\beta 1$ and $\alpha IIb\beta 3$. The GPIb-IX-V complex is composed of four distinct gene products, GPIbα disulfide-linked to GPIbβ, GPIX, and GPV (*2*, *3*). The sites responsible for vWF binding lie within the 293 N-terminal residues of GPIbα with a primary role for a disulfide-linked double loop domain located after seven leucine-rich repeats, although the latter may also intervene in forming the vWF binding pocket (*4*−*6*). The presence of leucine-rich repeats characterizes the GPIbα subunit as does tyrosine sulfation and a heavily glycosylated mucin core bridging the active sites and the transmembrane domain. Single leucine-rich repeats are also present in GPIX and GPIbβ while GPV has 15, and these are thought to have an important role in governing subunit structure.

BSS is an inherited bleeding disease symptoms of which include giant platelets and a small number of circulating platelets with defective platelet adhesion to vWF (*3*, *7*). Quantitative deficiencies of the GPIb-IX-V complex characterize this syndrome, and a nonfunctional complex is present in rare cases. A majority of the reported molecular defects in BSS concern the GPIbα gene, and give rise to a structurally modified or truncated protein with severely inhibited or absent expression of GPIbα on the platelet surface (*3*, *7*). This in turn leads to a much reduced level of surface expression of both GPIX and GPV. An example is an early reported Cys^{209} → Ser missense mutation where platelets and megakaryocytes totally lacked GPIbα and only had small residual intracellular pools of GPIX and GPV (*8*, *9*). Findings such as this suggested that the formation of a stable complex between GPIbα, GPIbβ, and GPIX was a necessary prerequisite for normal transport of each gene product through the membrane systems of the maturing megakaryocyte. It was soon recognized that genetic lesions

* To whom correspondence should be addressed. Telephone: 33.5.57.65.68.08. Fax: 33.5.57.65.65.31. E-mail: Alan.Nurden@cnrshl.u-bordeaux2.fr.

[‡] INSERM U311-Etablissement Français du Sang.

[§] Hôpital Cardiologique.

[||] CHU Timone.

[1] Abbreviations: vWF, von Willebrand factor; GP, glycoprotein; BSS, Bernard-Soulier syndrome; CHO, Chinese hamster ovary; ACD-A, acid-citrate-dextrose; RT, room temperature; MoAb, monoclonal antibody; PFA, paraformaldehyde; FITC, fluorescein isothiocyanate; FACS, fluorescence-activated cell sorting; MFI, mean fluorescent intensity; sulfo-NHS-LC-biotin, sulfosuccinimidyl-6-(biotinamido)-hexanoate; SDS−PAGE, SDS−polyacrylamide gel electrophoresis; PVDF, polyvinylidene difluoride; BSA, bovine serum albumin; HRP, horseradish peroxidase; DTT, dithiothreitol; ERGIC, ER−Golgi−intermediate compartment; ER, endoplasmic reticulum; LR, leucine-rich repeat.

10.1021/bi026213d CCC: $25.00
Published on Web 03/28/2003

within the GPIbβ and GPIX genes can also give rise to BSS. Transfection of heterologous cells with combinations of GPIbα, GPIbβ, and GPIX genes, mutated or not, showed that if complex formation did not occur, trafficking of the individual subunits was severely impaired (*10*−*13*).

Although the pathological effects of mutations in the GPIbα and GPIX genes have been well-studied, the influence of mutations in the GPIbβ gene on GPIb-IX maturation is less clear. Two early independent reports have associated heterozygous GPIbβ deficiencies with the Di George/velocardio-facial syndrome characterized by a microdeletion within 22q11.2 (*14*, *15*). The GPIbβ gene maps to this region. In the first such patient, one allele contained the deletion and in the second allele the GPIbβ gene contained a C to G transversion at the base 133 positions downstream of the transcription start site. The mutation changed a GATA consensus binding site, disrupting GATA-1 binding and decreasing promoter activity by 84% (*16*). In a second patient, the undeleted allele contained a translational frameshift and encoded a truncated and nonfunctional GPIbβ protein (*15*). Heterozygous and homozygous amino acid substitutions were then reported within the GPIbβ extracellular domain in the absence of Di George syndrome (*17*−*19*). These prevented surface expression of GPIb-IX when the mutated gene was coexpressed with the wild-type genes for the other subunits in heterologous cells. We now report a novel homozygous $Asn^{64} \rightarrow Thr$ mutation within the COOH flanking domain of the leucine-rich repeat of GPIbβ in a young Algerian boy with BSS. The effect of the mutant protein on the processing of wild-type GPIbα and GPIX was studied in detail following site-directed mutagenesis in Chinese hamster ovary (CHO) cells, and shown to result in GPIX instability as well as an incomplete maturation of the GPIbα subunit. GPIbβ therefore has a dual chaperone-like role in the biosynthetic pathway of this important adhesion receptor.

MATERIALS AND METHODS

Patient Information. The case under study is a 16-year-old Algerian boy living in France. He has a severe bleeding condition. His platelets are giant on peripheral blood smear, and the typical morphology of BSS was confirmed by electron microscopy (see patient S.B. in ref *20*). This included a rounded shape, with abundant vacuoles and abnormal zones of membrane complexes. His platelet count is low at $\approx 40 \times 10^3$ per μL. An unusual characteristic of this patient is a spontaneous agglutination when his platelets are stirred in EDTA or citrate-anticoagulated blood. This disappears after platelet washing. Bleeding has required transfusion therapy. In June 2001, testing his serum for anti-platelet antibodies revealed a strong antibody to GPIb-IX-V complexes of normal platelets. Blood samples from his father (H.B.), mother (D.B.), two brothers (Mo.B. and Me.B.), and a sister (A.B.) were sent from Algeria for DNA testing. Blood was also obtained for glycoprotein evaluation from H.B. and Mo.B. Patient S.B. has been studied by us on four occasions spread over several years. Control donors were normal hospital staff. All studies were performed with informed consent.

Platelet Isolation. Six volumes of blood was anticoagulated with 1 volume of ACD-A [38 mM citric acid, 61 mM trisodium citrate, and 136 mM glucose (pH 6.5)]. Blood from control donors was centrifuged at 250*g* for 15 min. Blood from the patient was subjected either to two cycles of low-speed centrifugation (15 min at 80*g* and then at 120*g*) to recover the maximum of platelets or to centrifugation across a Lymphoprep Ficoll gradient (Nycomed Pharma, Oslo, Norway) as described previously (*20*). PGE_1 (Sigma Chemical Co., St. Louis, MO), at a final concentration of 20 ng/mL, and apyrase (grade I, Sigma) at 25 μg/mL were added to the platelet-rich plasma (PRP). Unless otherwise stated, platelets were washed three times and resuspended at a final concentration of 10^8 per mL (patient) or 10^9 per mL (control) in a modified Tyrodes-Hepes buffer (*21*).

FACS Analysis of Platelets. Experiments were performed using PRP with or without prior fixation performed by incubating with 1% PFA for 30 min at RT (*8*, *21*, *22*). On one occasion, washed platelets were incubated at 37 °C for 10 min with or without 0.5 unit/mL α-thrombin (Ortho Diagnostic Systems, Raritan, NJ) prior to fixation (*21*). Incubation with MoAbs was according to our standard procedures (*22*, *23*). A range of murine MoAbs was used: AP-1 (from T. Kunicki, La Jolla, CA), AK2 (obtained from the Boston Workshop, 1994), SZ2 (Immunotech Coulter, Marseille, France), and ALMA.12 (all directed against the NH_2-terminal domain of GPIbα); Bx-1 and WM23 (from M. Berndt, Melbourne, Australia) (both recognizing the membrane proximal fragment of GPIbα); FMC25 (AMRAD Biotech, Boronia, Australia), ALMA.16, Beb-1 (5^{th} Workshop on Human Leukocyte Differentiation Antigens, Boston, 1994), and SZ1 (Beckman Coulter, Roissy, France) (all anti-GPIX); SW16 (from A. von dem Borne, Amsterdam, The Netherlands) (anti-GPV); Gi27 (from S. Santoso, Giessen, Germany) (anti-GPIbβ); Gi9 (Immunotech Coulter) (anti-α2β1); AP-2 (from T. Kunicki) (anti-αIIbβ3); and VH10 (anti-P-selectin). Where no citation is given, MoAbs were from the authors' laboratories. Antibodies were used at predetermined saturating concentrations as assessed for control platelets, and isotype murine IgG controls were also performed (*22*). Cell-bound IgG was detected using FITC-conjugated affinity-purified $F(ab')_2$ fragments of a sheep antibody to mouse IgG (AMRAD Biotech) (*22*, *23*). Samples were analyzed with a Becton Dickinson FACScan flow cytometer (Becton Dickinson Immunocytometry Systems, Le Pont de Claix, France) using LYSIS II software, and values for the mean fluorescent intensity (MFI) are given on an arithmetical scale (*22*). In each experiment, 10 000 platelets were analyzed.

Western Blotting of Platelet Extracts. Washed platelets from the patient, his father, and one brother (Mo.B.) as well as from control donors were solubilized by heating at 37 °C for 10 min in the presence of 1% SDS, 5 mM *N*-ethylmaleimide, and 3 mM EDTA (pH 7.0) (*23*). Electrophoresis was performed on 7 to 12% gradient gels. Proteins were transferred to a nitrocellulose membrane (*23*). Membranes were incubated with MoAbs to GPIbα (Bx-1), αIIb (SZ22, Immunotech Coulter), or β3 (XIIF9), and bound IgG was revealed using a HRP-conjugated antibody specific for mouse IgG (Jackson ImmunoResearch, West Grove, PA) either colorimetrically or by chemiluminescence (ECL Detection Kit, Amersham, Les Ulis, France).

Surface Biotinylation and Immunoprecipitation Procedures Using Platelets. After the first wash, platelets were incubated

with 0.5 mg/mL sulfo-NHS-LC-biotin (Pierce, Rockford, IL) for 30 min at 37 °C, and then washing was continued using the procedures described above. Immunoprecipitations were performed on platelet lysates. Samples of washed platelets (10^8 per mL) were incubated with an equal volume of NP-40 lysis buffer composed of 2% Nonidet P-40, 300 mM NaCl, 20 mM Tris-HCl, 1 mM PMSF, 10 mM EDTA, 2 mM Na_3VO_4, 20 μg/mL leupeptin (Sigma), 5 μg/mL pepstatin (Sigma), and 5 mM NaF. After 30 min on ice, lysates were precleared by centrifugation for 10 min at 10000*g*. Immunoprecipitations were carried out on the supernatants with 5 μg of WM23, a MoAb to GPIbα. After 2 h, a volume of protein G−Sepharose beads (Sigma) was added and the incubation continued for a further 4 h. The protein G−Sepharose beads were washed five times and the bound proteins recovered by SDS solubilization. Proteins were separated by SDS−PAGE on 7 to 15% gradient gels and transferred to a PVDF membrane. The membranes were blotted for Ibα using WM23 (0.5 μg/mL) or, for biotinylated glycoprotein, with horseradish peroxidase (HRP)-conjugated avidin (1:5000 dilution, Sigma). Bound IgG was revealed by chemiluminescence using a HRP-conjugated antibody specific for mouse IgG (Jackson ImmunoResearch).

Immunofluorescence Microscopy of Platelets. Platelets were fixed with 3.7% PFA for 30 min and allowed to sediment on glass slides coated with polylysine as described previously (*24*). Slides were saturated for 30 min with modified Tyrodes-Hepes buffer containing 1% BSA and then incubated with murine MoAbs to GPIbα (WM23, Bx-1, and AP-1), αIIb (SZ22, Immunotech Coulter), or β3 (XIIF9). After several washes, the FITC-labeled antibody to mouse IgG was added as in flow cytometry, and incubations were continued for an additional 1 h. After further washing had been carried out, mounting medium and antifading agent (Molecular Probes, Interchim, Montluçon, France) were added together with a coverslip. Controls were performed without the primary antibody. Cells were observed under a confocal microscope (Nikon Eclipse E800, Nikon, Champigny/Marne, France) (*24*).

DNA Extraction, Amplification, and Sequencing. DNA was extracted from 200 μL of citrated blood with a QIAamp Blood Kit (QIAGEN GmbH, Hilden, Germany). Amplification of GPIbα, GPIbβ, and GPIX was performed using two pairs of nested primers for GPIbα (P1 and P2 followed by P3 and P4) and GPIbβ (P5 and P6 followed by P7 and P8) and one pair of primers for GPIX (P9 and P10). GPIbα primers were P1 (2951−2980), P2 (5132−5104), P3 (3045−3068), and P4 (5034−5011) (GenBank entry M22403), GPIbβ primers P5 (12621−12646), P6 (13632−13607), P7 (12655−12680), and P8 (13596−13572) (GenBank entry AF006988), and GPIX primers P9 (675−698) and P10 (2298−2276) (GenBank entry M80478). Sequencing was carried out on PCR products using a DNA sequencing kit and an ABI PRISM 377 DNA sequencer (Perkin-Elmer, Foster City, CA) (*25*).

In Vitro Mutagenesis. Site-directed mutagenesis was performed by replacing the *Acc*I−*Sma*I (nucleotides 13120−13494) fragment of the GPIbβ cDNA cloned into the PDX expression vector by the equivalent fragment obtained by PCR amplification from the patient's genomic DNA. The cDNAs encoding each chain of the GPIb-IX complex were subcloned individually in the pDX expression vector (*26*). The pDX expression vector bears the prokaryotic ampicillin resistance gene, and eukaryotic gene expression is driven by the adenovirus major late promoter and the SV 40 enhancer. The pCDNA3 vector conferring G418 resistance was purchased from Invitrogen (San Diego, CA).

Cell Culture and Transfection. Cells of the CHO-K1 cell line were grown in Ham's F-12 medium (Gibco BRL, Life Technologies GmbH, Eggenstein, Germany) with 10% fetal bovine serum. Plasmids for transfection were purified using the Plasmid Maxi Kit (Qiagen). A fixed amount (150 ng) of each expression plasmid and 50 ng of pcDNA3 were used for the transfection performed using ExGen 500 (Euromedex, Strasbourg, France), according to the manufacturer's conditions. Briefly, plasmids were resuspended in 150 mM NaCl, and 5 μL of ExGen/μg of DNA was added. The mixture was added to a dish containing the CHO cells. After 3 h, the cells were washed and allowed to grow in F12 medium supplemented with 10% fetal calf serum (Gibco BRL). Three days after transfection, the cells were subjected to selection by G418 (400 μg/mL) (Boehringer-Mannheim). Cloning rings were used to isolate resistant clones 10 days after transfection. In "rescue" experiments with clones expressing β64Thr, cells were additionally treated with the pDX expression vector in the presence of ExGen and the cell population was analyzed after 48 h. Transient transfections were also performed using CHO cells stably expressing the GPIbα and GPIX subunits (CHO α-IX) and selected after transfection of the corresponding PDX plasmids and of pcDNA3, G418 selection, and cloning as described above.

FACS Analysis of CHO Cells Expressing Recombinant GPIb-IX. Cells (5×10^4 cells/point) were detached with EDTA, resuspended in PBS, fixed for 15 min at RT with 1% PFA in a final volume of 2 mL, and permeabilized or not with 1% saponin. They were then incubated with predetermined saturating concentrations of the primary MoAb for 30 min at 4 °C, washed, and incubated for 30 min at 4 °C in the dark with a 100-fold dilution of FITC-labeled goat anti-mouse IgG (Jackson ImmunoResearch). Samples were analyzed on a FACScalibur flow cytometer using Cell Quest software (Becton Dickinson Biosciences, Rungis, France). A rat monoclonal antibody (RAM.1) to the extracellular domain of GPIbβ was used in some experiments and detected with the DTAF-labeled goat antibody to rat IgG (Jackson ImmunoResearch) (*27*).

Immunoprecipitation and Western Blotting of Transfected CHO Cell Lysates. Cells (2×10^6 per point) were washed twice in PBS and resuspended in lysis buffer [PBS containing 1% Triton X-100, 1× protease inhibitor cocktail, and 2 μg/mL calpain inhibitor (Roche diagnostics GMBH, Mannheim, Germany)] for 20 min at 4 °C. The suspension was cleared by centrifugation at 80000*g* for 15 min at 4 °C. Supernatants were cleared twice for 1 h at 4 °C with 100 μL of protein G−agarose beads (Sigma) and incubated overnight at 4 °C with 10 μg/mL ALMA.12 and 100 μl of fresh protein G−agarose beads. After a rapid centrifugation, the beads were washed four times in lysis buffer. Immunoprecipitated proteins were solubilized by boiling for 5 min at 97 °C in Laemmli buffer containing (reduced) or not (nonreduced) 10 mM DTT and separated by SDS−PAGE on 7.5 to 15% gradient gels.

Proteins were transferred to Immobilon-P membranes (Millipore, Saint Quentin en Yvelines, France). After satura-

tion with 10% Genosys blocking solution (Sigma) in PBS containing 0.05% (w/v) Tween 20, the membrane was incubated for 30 min at RT with a 2000-fold dilution of polyclonal K5834, a rabbit anti-GPIb-IX complex antibody (provided by B. Steiner, Hoffmann-La Roche, Basel, Switzerland). The membrane was washed four times for 30 min in a 0.05% PBS/Tween mixture and then incubated for 1 h at RT with a 10000-fold dilution of HRP-conjugated goat anti-rabbit IgG in PBS containing 0.05% Tween 20. After extensive washing had been carried out, the bound antibody was revealed by chemiluminescence.

Immunoprecipitation of Metabolically Labeled Proteins. Cells (5×10^7 per mL) were incubated twice in 50 mL of cysteine- and methionine-free RPMI medium (ICN, Costa Mesa, CA) without fetal calf serum for 30 min at 37 °C. The cells were then pulse-labeled for 15 min at 37 °C with 3 mCi (111 MBq) of a mixture of [^{35}S]methionine and [^{35}S]-cysteine (Amersham Pharmacia Biotech) (*28*). The cells were diluted in 10 volumes of ice-cold PBS, washed once, and chased for different amounts of time at 37 °C in RPMI containing 10% dialyzed fetal calf serum. At each chase time, cell samples were washed twice in ice-cold PBS and lysed in buffer I [20 mM Tris (pH 7.5), 150 mM NaCl, 5 mM EDTA, 0.2% BSA, 1% Triton X-100, and a 1× protease inhibitor cocktail]. Cell lysates were clarified by incubating them twice with 100 μL of protein G−agarose beads for 1 h at 4 °C. The lysates were then incubated overnight at 4 °C with 10 μg of the chosen antibodies and 100 μL of fresh protein G−agarose beads. After centrifugation, the bead pellets were washed four times in buffer I containing 0.1% Triton X-100, resuspended in Laemmli buffer in the presence or absence of 10 mM DTT, and boiled for 5 min. Proteins were resolved by SDS−PAGE on 7.5 to 15% gradient gels, and radiolabeled proteins were detected by autoradiography.

Confocal Microscopy. CHO cells were seeded on polylysine-coated coverslips for 15 min at RT. After washing had been carried out, the cells were fixed with 3% PFA and permeabilized with 0.05% saponin in a blocking solution composed of PBS containing 0.2% BSA and 1% goat serum (*28*). In addition to MoAbs to GPIb-IX, antibody markers to specific intracellular membrane fractions were also used. These included GS28, a MoAb against GS28 (a specific cis-Golgi marker) (StressGen Biotechnologies, Victoria, BC); Gi93, a MoAb recognizing an ER−Golgi−intermediate compartment (ERGIC, from M. Bornens, Institut Curie, Paris, France); and a polyclonal antibody to calnexin, a marker of the ER (Chemicon, Temecula, CA). Antibodies were incubated in blocking solution for 45 min at RT as follows: ALMA.12 (Al.12), Gi27, Gi93, and GS28 at 4 μg/mL and polyclonal anti-calnexin at 1 μg/mL. When not directly labeled with a fluorophore, murine MoAbs were revealed with GAM-Cy3 (Jackson ImmunoResearch) or GAM-Alexa 488 (Molecular Probes, Eugene, OR) at a 1:400 dilution. Anti-calnexin was revealed with a donkey anti-rabbit antibody coupled to Texas Red (Jackson ImmunoResearch). Labeled cells were examined under a Zeiss laser scanning microscope (LSM 410 invert) equipped with a planapo oil immersion lens (63×, n.a. = 1.4) as described elsewhere (*28*).

RESULTS

FACS Analysis of Components of the GPIb-IX-V Complex on the Patient's Platelets. In a preliminary report, we had previously noted that washed platelets from patient S.B. expressed residual GPIbα as detected by a single MoAb, Bx-1 (*20*). We now describe a more comprehensive FACS analysis of the surface expression of GPIb-IX-V on his platelets. Typical fluorescence histograms obtained for PFA-fixed normal and S.B. platelets are shown in Figure 1. Residual binding of Bx-1 was again seen and was also observed for WM23. Nevertheless, binding of the two MoAbs showed different characteristics. Thus, in the illustrated experiment, Bx-1 recognized 63% of the platelets with an MFI of 83 compared to an MFI of 170 for the control. WM23 bound to virtually all platelets but with an MFI of 34. In contrast, binding of AP-1 remained at background levels as did those of SZ2 and AK2 (not shown). AP-1 and AK2 recognize exposed conformation-dependent epitopes on GPIbα, while SZ2 requires tyrosine sulfation (Table 1). Significantly, MoAbs to GPIX, such as FMC25, SZ1 (both illustrated in Figure 1), and Beb-1 (not shown), all bound minimally to the patient's platelets. GPV was clearly present on ~50% of the platelets. All platelets from S.B. abundantly bound AP-2, a MoAb recognizing the αIIbβ3 integrin (Figure 1), and also bound Gi9 (anti-α2β1) (not shown). The above results were reproducible, and a positive binding of Bx-1 and WM23 to platelets of the patient was seen on four occasions spread over a period of 4 years. Results were unaffected by how the PRP was prepared for the patient (see Materials and Methods) or by PFA fixation, unfixed platelets in PRP showing a comparable reactivity. After stimulation with a large dose of α-thrombin (0.5 unit/mL), washed platelets from S.B. underwent secretion after which P-selectin was homogeneously expressed within the total population (not shown).

Immunofluorescence Microscopy. PFA-fixed platelets from the patient and controls were observed in a confocal microscope after labeling with MoAbs WM23, AP-1, and SZ22 as in the flow cytometry experiments. As can be seen in Figure 2A, normal platelets were uniformly recognized by all three MoAbs, whereas platelets from the patient were not recognized by AP-1. Platelets with an "annular" fluorescence were clearly seen with WM23 in the patient's population, confirming a plasma membrane localization for the recognized protein. No labeling was seen with FMC25 to GPIX (data not shown). SZ22, a MoAb to the αIIb subunit of the αIIbβ3 integrin, gave strong and homogeneous labeling of the patient's platelets. The negative result with AP-1 additionally provides a control that the patient's platelets were not binding the secondary FITC-labeled antibody alone.

Biotinylation of Platelets from S.B. and Immunoprecipitation with WM23. Washed platelets from the patient and a control donor were surface biotinylated; lysates were obtained and incubated with WM23 before addition of protein G−Sepharose beads. As shown in Figure 2B, whereas biotinylated GPIbα was immunoprecipitated from the control platelets, there was no band in the 130 kDa position corresponding to this protein in the patient's sample. In contrast, a single biotin-labeled band was present at 66 kDa. An identically migrating band and one of 56 kDa were also

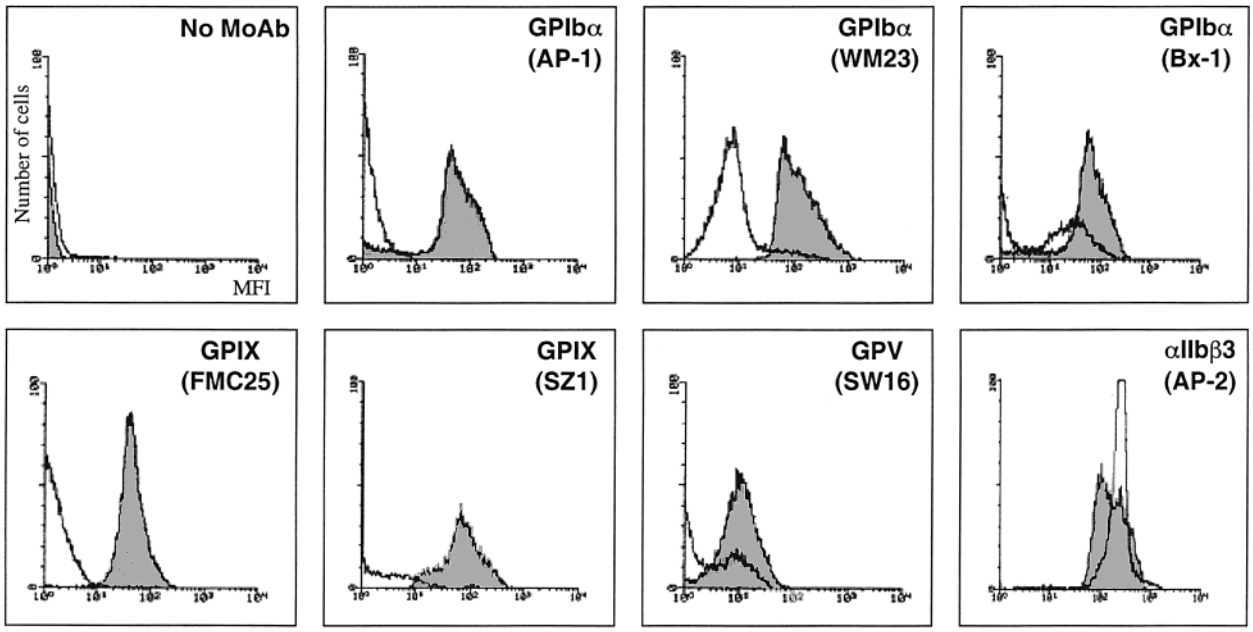

FIGURE 1: FACS analysis of platelets from patient S.B. Platelets in PRP from the patient and a control were fixed with PFA prior to incubation with MoAbs to the N-terminal domain of GPIbα (AP-1), the mucin-like core region of GPIbα (Bx-1 and WM23), GPIX (FMC25 and SZ1), GPV (SW16), and αIIbβ3 (AP-2). Bound IgG was detected using the FITC-labeled second antibody and flow cytometry. The results showed that the patient (white histograms) as compared to the control (gray histograms) possessed a variant form of BSS with residual and structurally abnormal GPIbα variably detected by MoAbs to this subunit, with residual GPV but lacking the GPIX component of the complex. A control incubation with the FITC-labeled second antibody alone is also shown (no MoAb).

Table 1: Specificity of the MoAbs to GPIbα Used in This Study[a]

MoAb	specificity	ref
AP-1	COOH flanking and leucine-rich region	*2*
AK2	residues 36−59 of a leucine-rich region	*2*
SZ2	sulfated tyrosine residues 269−282	*2*
ALMA.12	NH_2-terminal 45 kDa fragment	*26*, *28*
WM23	macroglycopeptide	*2*
Bx-1	macroglycopeptide	*21*, *28*

[a] The macroglycopeptide refers to a soluble protease-released fragment of the extracellular domain of GPIbα that contains the mucin-rich core. The 45 kDa fragment is terminal to the macroglycopeptide and contains the leucine-rich repeats.

observed on the control pattern. Low-molecular mass bands probably corresponding to GPIbβ and GPIX were visible on the control platelet pattern but not detected for the patient. None of the bands were seen in the absence of WM23.

Family Studies. FACS analysis using the MoAb, AP-1, initially confirmed that platelets from the patient's father (H.B.) and a brother (Mo.B.) expressed intermediate amounts of GPIbα. This was confirmed by Western blotting using platelet lysates when the level of relative staining of the GPIb band was specifically reduced compared to the αIIb and β3 bands on incubating membranes with a mixture of MoAbs to each GP followed by HRP-labeled anti-mouse IgG and colorimetric detection (not illustrated).

Sequence Analysis of the Components of the GPIb-IX Complex. The genes encoding GPIbα, GPIbβ, and GPIX were amplified using DNA from the patient's leukocytes and directly sequenced. No mutations were found in the GPIbα or GPIX genes, but the GPIbβ gene contained a homozygous A to C transversion at position 919 according to the nomenclature of Yagi et al. (*29*). The substitution led to an asparagine (Asn) to threonine (Thr) amino acid change at position 64 of the mature polypeptide (Figure 3A). Both parents and two brothers were heterozygous for the substitution (Figure 3B). A sister did not have the mutation. The Asn → Thr change fell within the COOH region flanking the LR motif of GPIbβ (Figure 3C). Alignment of corresponding sequences from other subunits of the GPIb-IX-V complex and from selected members of the LR family with a C-terminal flanking Cys cluster (*30*) revealed that the Asn mutated in patient S.B. is highly conserved (Figure 3D).

Expression of the Mutant GPIb-IX Complex in CHO Cells. To test whether the mutation of the GPIbβ gene causally resulted in a loss of GPIb-IX expression as observed in the patient's platelets, the β64Thr mutation was inserted in a GPIbβ expression vector and cotransfected in CHO cells with wild-type GPIbα and GPIX. None of the G418 resistant clones was found to be positive for GPIb-IX surface expression by FACS analysis. Two clones were selected on the basis of RT-PCR positive responses for the GPIbβ, GPIbα, and GPIX transcripts (data not given). One stable clone (β64Thr-CHO) was chosen, as was a clone encoding the three wild-type genes (β64Asn-CHO). As shown in Figure 4, FACS analysis confirmed that both GPIbα and GPIX were abundantly detected at the surface of β64Asn-CHO cells [the anti-GPIbβ MoAb used, Gi27, fails to have access to its epitope on intact cells being directed against an intracellular domain (*30*)]. FACS analysis of β64Thr-CHO cells showed that none of the gene products reached the surface (not illustrated). However, as presented in Figure 4, FACS analysis after membrane permeabilization with saponin gave positive responses for GPIbα with WM23 and ALMA.12. Results remained negative for AP-1 (not illustrated) and for two different GPIX MoAbs (FMC25 and ALMA.16). Positivity was also detected for GPIbβ (Gi27) (see the arrow on the histogram).

When the stable β64Thr-CHO clone was further transiently transfected with the wild-type human GPIbβ gene, FACS

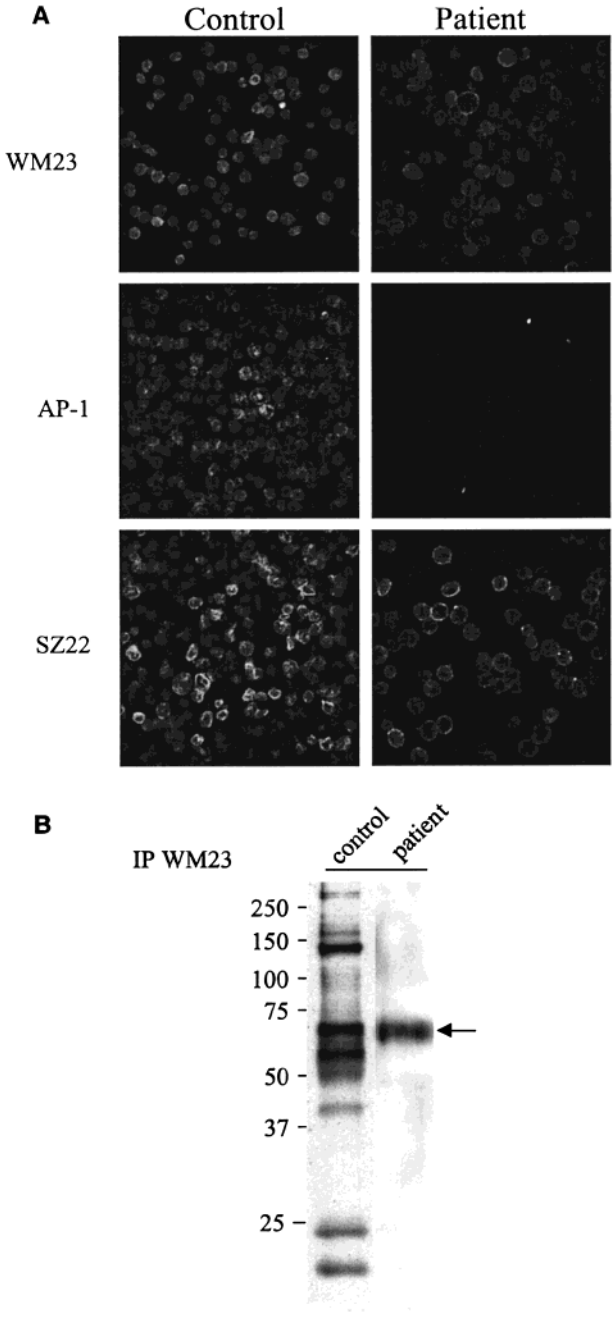

FIGURE 2: Fluorescence microscopic detection of GPIbα and analysis of surface-biotinylated platelets. (A) PFA-fixed platelets from patient S.B. and a control were examined with a confocal microscope after incubation with WM23, AP-1, and SZ22, a MoAb to αIIb. Bound mouse IgG was detected using the FITC-labeled second antibody. Note the residual GPIbα in S.B. platelets detected by WM23 but not AP-1. (B) Surface-biotinylated platelets were lysed with Nonidet P-40 and immunoprecipitated with WM23. After electrophoresis and transfer, biotinylated proteins were detected with HRP-bound avidin. Results show a single band at $\approx$66 kDa for the patient.

analysis 48 h after transfection showed that the biosynthesis of normal GPIbβ led to surface expression of GPIbα in the cells as located using ALMA.12 (ratio MFIβ64Thr + wild-type βAsn/β64Thr = 1.61). As a control, β64Thr-CHO cells transiently transfected with the GPIX gene in place of the wild-type human GPIbβ gene failed to express surface GPIbα. Nevertheless, the amount of expression in these experiments remained weak. So we also transiently transfected a stable CHO cell line preselected for its capacity to express GPIbα and, to a lesser extent, GPIX (Figure 5A). One goal was to rule out possible phenotypic drift in the β64Thr-CHO clone unrelated to the mutation. Transient expression of wild-type GPIbβ in the CHO α-IX cells allowed for efficient GPIbβ-IX expression in $\sim$30% of the cells both inside the cells (Figure 5B) and on the surface (data not shown). Transfection of β64Thr failed to sustain GPIX expression in the cells. Thus, the Asnβ64 to Thr substitution clearly has a major impact on GPIX expression. GPIbβ64Thr itself was not recognized by RAM.1.

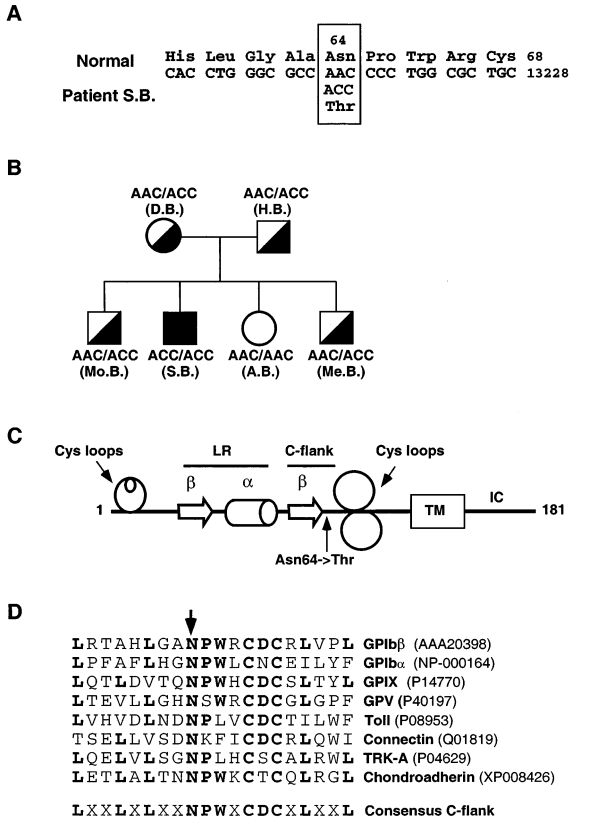

FIGURE 3: Sequence analysis of the GPIbβ gene. (A) A homozygous A to C transition at nucleotide 919 of the GPIbβ gene was identified for the patient S.B. The mutation led to an Asn^{64} to Thr substitution. (B) This mutation was present in a heterozygous form in the father and mother, confirming a classic mendelian autosomal recessive inheritance. (C) The Asn^{64} $\rightarrow$ Thr change occurred within the COOH region flanking the LR motif and the Cys cluster of GPIbβ. (D) The substitution (vertical arrow) occurs in a highly conserved region in members of the leucine-rich family with a C-terminal flanking Cys cluster (*30*).

The GPIbβ Asn^{64} $\rightarrow$ Thr Mutation Resulted in Abnormal Maturation of GPIbα. SDS−PAGE of β64Asn-CHO cell lysates followed by Western blotting with a polyclonal antibody prepared against purified GPIb-IX complexes (Figure 6A) clearly allowed the identification of a large 130 kDa GPIbα band after disulfide reduction (left panel) as well as the fast migrating GPIX and GPIbβ bands (right panel). In contrast, the results obtained for β64Thr-CHO cell lysates showed a prominent band at $\approx$66 kDa and no band at 130 kDa. While a band corresponding to GPIbβ continued to be seen, there was no band in the position of GPIX. Immunoprecipitation of Triton X-100 lysates from β64Thr-CHO cells with ALMA.12 followed by Western blotting with a polyclonal antibody raised against GPIb-IX also failed to reveal

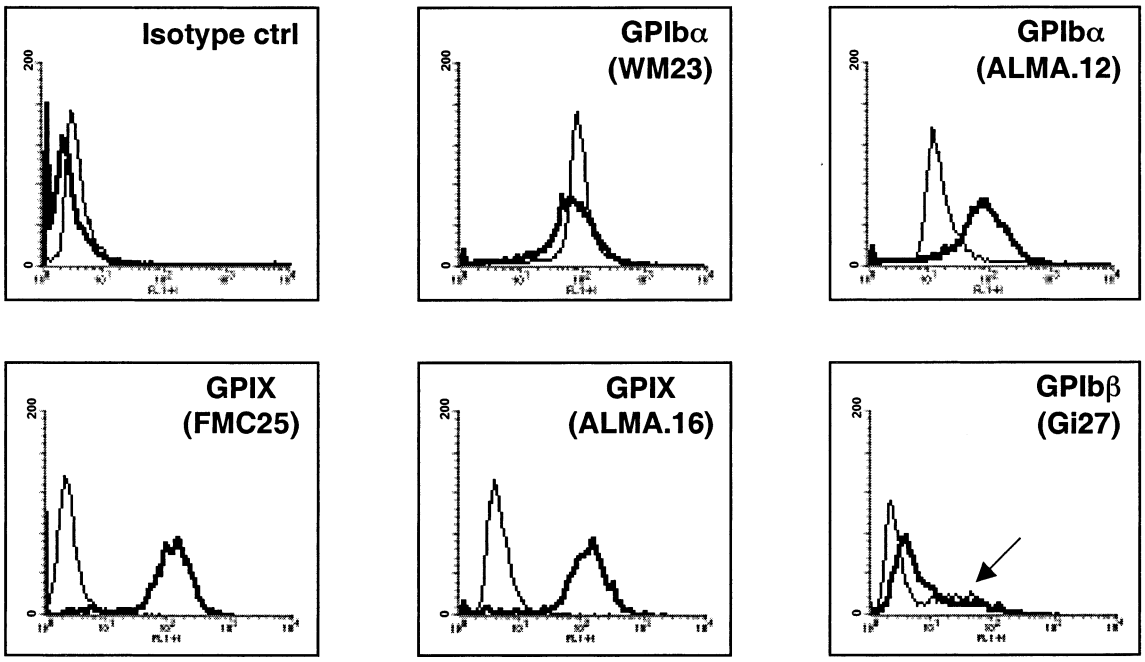

FIGURE 4: FACS analysis of the GPIbβThr64 substitution on GPIb-IX expression in a CHO cell line. Subunit surface expression was examined on PFA-fixed cells expressing the wild-type GPIb-IX complex (β64Asn-CHO). Note the abundant expression of GPIb-IX on the surface of the cells transfected with the three wild-type genes (histograms with thick lines). PFA-fixed cells transfected with wild-type GPIbα and GPIX genes and the GPIbβ gene containing the patient's mutation (β64Thr-CHO) were analyzed in parallel (histograms with thin lines). As none of the gene products reached the surface (not shown), results are presented after saponin permeabilization which shows an intracellular pool recognized by MoAbs against GPIbα and GPIbβ (see the arrow) but not against GPIX.

a band of the expected size for GPIbα under reducing conditions, and an ≈66 kDa band was again obtained (Figure 6B). On the basis of the Gi27 reactivity by FACS (Figure 4), the presence of GPIbβThr64 had been established in the permeabilized cells. The fact that the ≈66 kDa band was again revealed under nonreducing conditions confirmed that it was not disulfide-linked with GPIbβ when a mass of ≈90 kDa would be predicted. This was additionally confirmed by the inability of Gi27 to co-immunoprecipitate the abnormal GPIbα and its ability to do it for the wild-type subunit (not shown).

Biosynthetic studies were next performed to assess a possible maturation defect in the GPIbα subunit. β64Thr-CHO cells were pulse-labeled with [^{35}S]Met and Cys and immunoprecipitated with ALMA.12 (Figure 6C). At early chase times, a 66 kDa band was detected which only slightly increased in molecular mass during a 4 h chase. No increase in molecular mass was observed under nonreducing conditions, indicating again a lack of association with GPIbβ. In contrast, for β64Asn-CHO cells, a band representing immature GPIbα and migrating at ~70 kDa was progressively replaced by mature GPIbα (Figure 6D). Here, molecular mass changes under nonreducing conditions were consistent with disulfide-linked complex formation with GPIbβ even for the immature form. The fact that wild-type immature GPIbα had a slightly slower migration than the equivalent band obtained for β64Thr-CHO cells suggested that the latter also possessed a modified initial glycosylation.

Fluorescence Microscopy of Transfected CHO Cells. The subcellular distribution of GPIbα and GPIbβ in β64Thr-CHO cells was compared to that observed in β64Asn-CHO cells, i.e., cells transfected with wild-type genes. In single labeling experiments, GPIbα and GPIbβ were found intracellularly in β64Thr-CHO cells with a fine vesicular appearance (Figure 7). The presence of the mutated subunit confirms the FACS analysis performed earlier. Again, GPIX was not detected, and little reactivity was seen with AP-1, directed against the LR region of GPIbα (not illustrated). The labeling with ALMA.12 contrasted with the annular peripheral staining for GPIbα in β64Asn-CHO cells. Comparison with markers of the ER, ERGIC, and Golgi compartments indicated that the labeling patterns for GPIbα and GPIbβ in β64Thr-CHO cells more closely matched that of the ER and were clearly distinct from that visualized with the ERGIC and Golgi markers where a more punctuate fluorescence was observed.

DISCUSSION

It is now well-established that GPIbα, GPIbβ, GPIX, and GPV are expressed as a multiprotein complex in platelets (data reviewed in ref *2*). Early interactions between the individual subunits are vital for their processing and transport to the cell surface. A novel way of studying these interactions is through the BSS, an inherited disorder in which natural mutations in the GPIbα, GPIbβ, and GPIX genes affect the maturation and processing of the adhesion receptor. An exception is GPV, which although its level of platelets is severely decreased in BSS patients lacking GPIb-IX has been reported to be independently expressed on transfected cells (*31*). Nevertheless, expressed GPV appears to require the other three subunits for correct surface stability. The fact that GPV-deficient platelets in transgenic mice have a normal ultrastructure and size, have a full surface expression of GPIb and GPIX, and show none of the platelet function deficiencies normally associated with BSS suggests that defects of the GPV gene are unlikely to be a cause of human BSS (*32*, *33*). For these reasons, our studies have focused on the assembly of the GPIbα, GPIbβ, and GPIX subunits.

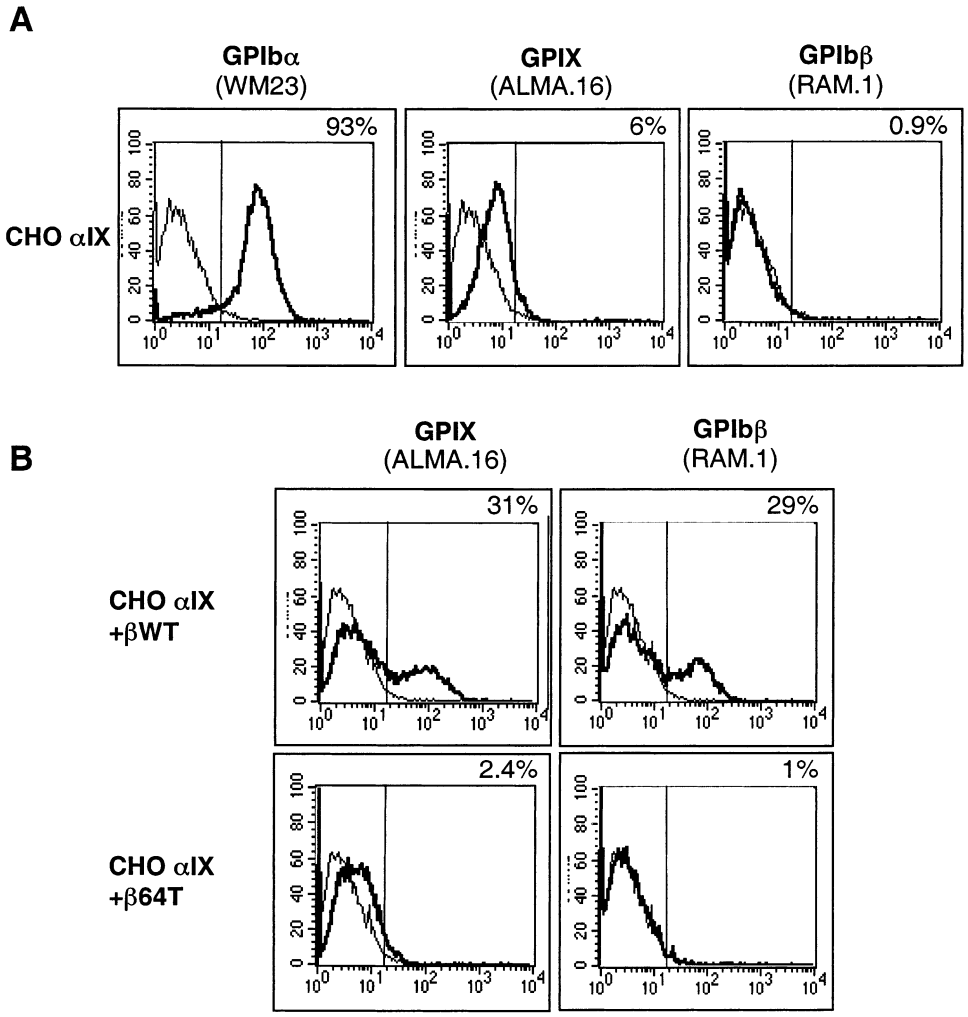

FIGURE 5: Effect of the GPIbβThr64 substitution on transient expression of GPIX in CHO cells. A subcloned CHO α-IX cell line stably expressing GPIbα and GPIX (A) was transiently transfected with wild-type GPIbβ or with GPIbβ64Thr and analyzed by FACS after saponin permeabilization for GPIX with ALMA.16 and for GPIbβ with RAM.1 (B). Note that efficient expression of GPIX and GPIbβ was seen with the wild type, but that GPIX was not enhanced in the presence of GPIbβ64Thr which was itself not recognized by RAM.1. Isotype controls are given (thin lines).

Characterizing the molecular defect of our BSS patient revealed a novel homozygous GPIbβ missense mutation with autosomal recessive inheritance. The possession of a single affected allele by both parents, together with an absence of associated skeletal defects in the patient, permitted us to exclude the involvement of Di George/velo-cardio-facial syndrome. In three other BSS patients, a single defective GPIbβ allele was associated with a second allele containing a microdeletion within 22q11.2, the site for the location of the GPIbβ gene, and typical of Di George syndrome (*14*, *15*, *34*). The defects in these patients involved loss of a GATA-1 binding site in the GPIbβ promoter (*14*), a frameshift leading to a stop codon (*15*), and a missense mutation (*34*); thus, they are clearly unrelated. The fact that our patient did not have this association is thus worthy of comment. Transfection experiments involving the preparation of stable CHO cells expressing wild-type GPIbα, wild-type GPIX, and wild-type GPIbβ or GPIbβ64Thr showed that the homozygous mutation detected in our patient fully explained the BSS phenotype. Transient expression rescue experiments involving the introduction of wild-type GPIbβ in β64Thr-CHO cells reinforced this conclusion. Experiments were then performed to explain how this mutation interfered with GPIb-IX complex maturation.

Flow cytometry, confocal microscopy, and Western blotting confirmed that GPIbβ64Thr was present in transfected CHO cells but showed the mutated protein to be retained in internal compartments. A comparison with other intracellular markers revealed a pattern of fluorescence more typical of the ER rather than of ERGIC or the cis-Golgi apparatus. This implies an early block within the processing of this subunit. Although GPIbα was present, it had a much lower molecular mass (66−70 kDa) in the GPIbβ64Thr-CHO cells. It has previously been shown that GPIbα normally forms a complex with GPIbβ and GPIX within the ER prior to its transport into the Golgi cistaernae (*12*, *26*). Immunoprecipitating GPIbα in GPIβ64Thr-CHO cell lysates with ALMA.12 resulted in no detectable coprecipitation of GPIbβ as indicated by the lack of a change in the migration of GPIbα from the nonreduced to the reduced state. GPIbβ attaches to GPIbα through a disulfide linking Cys residues proximal to but extracellular to the transmembrane domains. Therefore, one possibility is that the GPIbβAsn64 → Thr substitution interferes with the conformation of Ibβ so that this disulfide

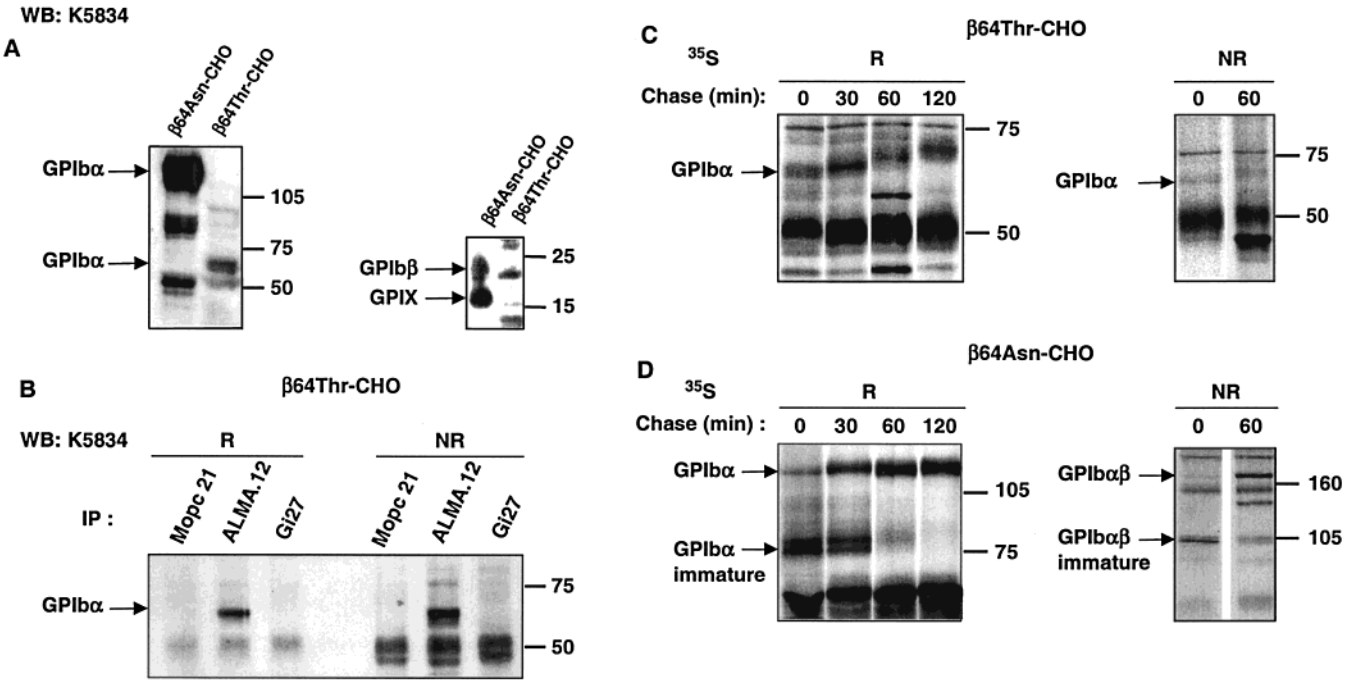

FIGURE 6: Effect of the GPIbβThr64 substitution on GPIb-IX maturation in a CHO cell line. (A) SDS-soluble extracts from β64Asn-CHO and β64Thr-CHO cells were subjected to SDS−PAGE after disulfide reduction and transferred to a nitrocellulose membrane prior to being probed with a rabbit antibody (K5834) prepared against isolated GPIb-IX. The presence of βThr64 led to marked changes in the maturation of GPIbα (left panel), while no GPIX was detected (right panel). (B) Triton X-100 extracts from β64Thr-CHO cells were immunoprecipitated with ALMA.12 (anti-GPIbα), Gi27 (anti-GPIbβ), or Mopc21 (control mouse IgG) followed by SDS−PAGE under both reducing (R) and nonreducing (NR) conditions and immunoblotting using the antibody K5834 to GPIb-IX. The results confirmed that a low-molecular mass form of GPIbα was immunoprecipitated by ALMA.12 and that βThr64 was not disulfide-linked to GPIbβ. (C) To follow the maturation of GPIbα, β64Thr-CHO cells were metabolically labeled with ^{35}S and pulse-chased for 2 h. Time-dependent changes in GPIbα maturation confirmed the presence of an $\approx$66 kDa component immunoprecipitated by ALMA.12 whose apparent size increased by 4 kDa during a 2 h chase. No molecular mass changes were observed under nonreducing conditions. (D) In contrast, in control experiments using β64Asn-CHO cells, GPIbα progressively matured to a 130 kDa product. Furthermore, increased molecular masses under nonreducing conditions indicated disulfide association of mature and immature GPIbα to GPIbβ.

cannot form. Structural considerations support this hypothesis. The mutation occurs in the COOH region flanking the single LR element of the subunit (Figure 3). From analysis of other LR proteins, this region could be viewed as a half-repeat with a β-strand predicted structure (*30*, *35*, *36*). The mutated Asn occupies a conserved position in the flanking region and may affect the packing and stability of the LR motif. This assumes that a single LR motif by itself would adopt the conformation observed in the crystallized proteins which have multiple repeats and an α-helix structure. Within LR repeats with a β-loop−helix motif, a conserved Asn forms hydrogen bonds with main chain atoms in its own repeat and with those in the preceding repeat, and a similar function could be proposed for residues in the flanking region. GPIbβAsn64 is also located close to a CDC motif thought to engage in disulfide bond formation, giving the double-loop structure in the extracellular membrane proximal domain of GPIbβ (*29*). Thus, there are several ways in which the presence of GPIbβThr64 could interfere with efficient bond formation, leading to an unstable complex.

The apparent molecular mass of the residual GPIbα ($\approx$66 kDa) detected in β64Thr-CHO cells is similar to that previously shown to represent an intermediate form of maturing GPIbα (*12*, *28*). This was confirmed in the control pulse chase experiments where the mass increased by only $\approx$4 kDa over a 4 h period. This form probably represents partially N-glycosylated GPIbα that has not undergone O-glycosylation, a process occurring in the Golgi apparatus and which accounts for approximately 40% of the mass giving GPIbα its characteristic mucin-like structure (reviewed in ref *2*). In addition, a lack of reactivity with the MoAb, SZ2, suggests that tyrosine sulfation of GPIbα was also defective. The implication is that formation of the GPIbα−GPIbβ disulfide is required for the maturation and processing of GPIbα from an early stage. BSS variant Nancy I refers to a patient with a deletion of Leu^{179} in the seventh leucine repeat of GPIbα (*25*). Intriguingly, when GPIb$\alpha\Delta$Leu was coexpressed in CHO cells with wild-type GPIbβ and GPIX, all three gene products reached the surface but GPIb$\alpha\Delta$Leu was found in smaller amounts and had a major O-glycosylation defect with a molecular mass of ~90 kDa (*26*). This molecular mass was nonetheless greater than that seen for CHOβ64 cells, suggesting that residual GPIbα in the CHOβ64 cells had more severe post-translational deficiencies. Significantly, in the GPIb$\alpha\Delta$Leu model, GPIb$\alpha\Delta$LeuβIX and GPIbβIX complexes were both detected, showing that the glycosylation defect per se did not totally abrogate complex formation or processing. Thus, the GPIbβ64Asn → Thr substitution leads to more profound abnormalities.

GPIX was not detected in CHO cells transfected with wild-type GPIbα, GPIX, and GPIbβ64Thr genes. GPIX is known to associate at least in part with GPIbα by way of GPIbβ, although a direct interaction may also occur (*11*, *12*). Site-directed mutagenesis has been used to evaluate the effect of Asp^{21} → Gly and Asn^{45} → Ser substitutions in GPIX on the surface expression of GPIbα in CHO cells (*13*). Unlike wild-

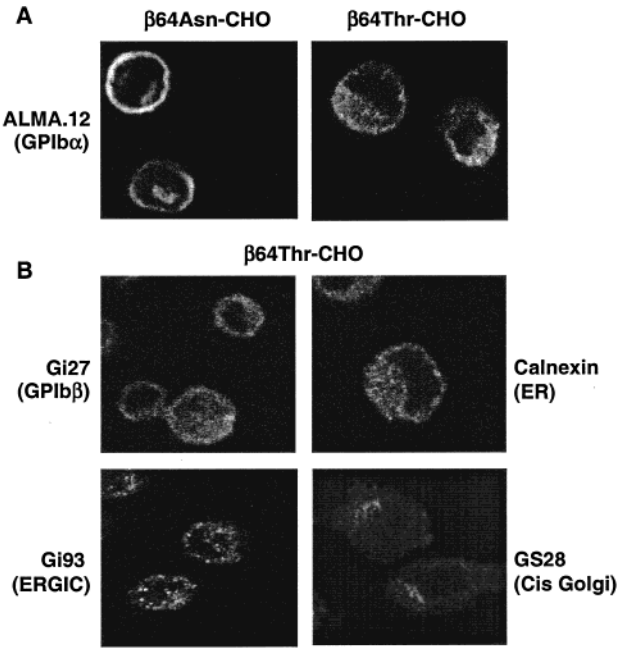

FIGURE 7: Fluorescence microscopy showing the influence of βThr64 on the localization of GPIbα and GPIbβ in a CHO cell line. β64Asn-CHO and β64Thr-CHO cells were immobilized on polylysine-coated coverslips, fixed, permeabilized, and singly labeled with the indicated MoAbs as described in Materials and Methods. The cells were analyzed by immunofluorescence confocal microscopy using filters for Cy3, Alexa-488, or Texas red as required. (A) In β64Asn-CHO cells, GPIbα labeling was mainly associated with the plasma membrane. In contrast, labeling was mainly intracellular in β64Thr-CHO cells with a fine vesicular appearance. (B) A similar labeling was observed in β64Asn-CHO cells for GPIbβ and was compared with that for markers of the ER, ERGIC, and Golgi.

type GPIX, neither of the mutants was able to bring GPIbα onto the cell surface despite their presence in small amounts in the intracellular compartment. Furthermore, although cotransfection of wild-type GPIX with GPIbβ resulted in the appearance of some GPIX on the CHO cell surface, neither of the GPIXGly^{21} and -Ser^{45} mutants reached the cell surface in appreciable quantities. Our studies would suggest that GPIbβ64Thr is unable to form a complex with GPIX and that the interaction between these two subunits is highly susceptible to changes in the conformation of the extracellular domains of these two subunits. This conclusion was reinforced by transient expression experiments using CHOα-IX cells where wild-type GPIbβ but not GPIbβ64Thr markedly enhanced GPIX expression. One hypothesis is that single LRR-containing proteins such as GPIbβ and GPIX need to associate via their repeat to form a multi-LR stable structure. Our failure to detect GPIX in the presence of GPIbβ64Thr suggests that alone it is highly susceptible to proteolytic degradation. Thus, the patient's mutation in GPIbβ exercises dual effects, affecting both the stability of GPIX and the maturation of GPIbα.

Other coding mutations in the GPIbβ gene in BSS have stressed the importance of a functional GPIbβ for GPIb-IX expression but have shed little light on the mode of action of GPIbβ. Kunishima et al. (*17*) reported two heterozygous missense mutations (Tyr^{88} → Cys and Ala^{108} → Pro). However, this Japanese compound heterozygote showed some unusual characteristics. First, FACS analysis showed that GPIbα and GPIX were expressed at decreased but readily detectable levels on the platelets and GPV approached normal density. Both GPIX and GPIbβ were coprecipitated with GPIbα, albeit at a concentration much lower than normal. It was subsequently shown that the Tyr^{88} → Cys substitution suppressed the expression of GPIb-IX complexes in transiently transfected 293T cells (*37*). A homozygous Pro^{74} → Arg mutation in the GPIbβ gene led to the absence of GPIbβ from platelets of a young Japanese girl despite a normal transcription (*18*). Flow cytometric analysis showed that the levels of surface expression of GPIbα and GPIX were severely reduced. Transient transfection in 293T cells showed that the Pro^{74} → Arg substitution was responsible for the BSS phenotype, but the mechanism behind its effect was not elucidated.

A unique finding in CHO cells expressing GPIbβ64 was an immature form of GPIbα noncomplexed with GPIbβ. Pulse chase studies in the presence of ^{35}S-labeled amino acids confirmed this to be an incompletely mature protein rather than a degraded GPIbα. A similar low-molecular mass form of GPIbα was also present in platelets, albeit in small amounts and with a heterogeneous distribution in the total cell population. Significantly, not all MoAbs to GPIbα recognized this immature form of GPIbα which was insensitive to AP-1, which blocks the binding of vWF to GPIb-IX, and recognizes a conformation-sensitive epitope within the terminal 45 kDa sequence and to SZ2 whose binding requires sulfated tyrosine residues at the carboxyl terminus of the same sequences. Experiments with surface-biotinylated platelets and fluorescence microscopy confirmed that some noncovalently linked GPIbα had been transported to the surface membrane. Why then were small amounts of immature GPIbα present alone on the platelets of patient S.B. but not on transfected CHO cells? This may reflect profound differences in the way membranes are processed in megakaryocytes and/or surface targeted when new platelets are formed, processes that are abnormal in BSS (*38*). Significantly, HEL cells with some megakaryocytic markers express in their surface membrane a similar immature form of GPIbα in the absence of GPIbβ or GPIX (*39*). As ER has recently been shown to possess unexpected pluripotent fusion properties and to be involved in cell trafficking processes (*40*), this is an important area for further study.

In conclusion, our studies mean that GPIbβ has a dual role in the maturation and trafficking of GPIbα. By interacting with GPIX, it stabilizes the latter so that the complex acts as a chaperone by guiding the transport of GPIbα through the membrane systems of the maturing megakaryocyte and onto the surface of newly formed platelets. Second, the covalent association of GPIbβ with GPIbα ensures the maturation of GPIbα and its O-glycosylation, in so doing inducing long-range conformational changes that render the vWF binding sites functional.

REFERENCES

1. Kulkarni, S., Dopheide, S. M., Yap, C. L., Ravanat, C., Freund, M., Mangin, P., Heel, K. A., Street, A., Harper, I. S., Lanza, F., and Jackson, S. P. (2000) *J. Clin. Invest. 105*, 783−791.
2. Berndt, M. C., Shen, Y., Dopheide, S. M., Gardiner, E. E., and Andrews, R. K. (2001) *Thromb. Haemostasis 86*, 178−188.
3. Lopez, J. A., Afshar-Kharghan, V., and Berndt, M. C. (1998) *Blood 91*, 4397−4418.
4. Vasudevan, S., Roberts, J. R., McClintock, R. A., Dent, J. A., Celikel, R., Ware, J., Varughese, K. I., and Ruggeri, Z. M. (2000) *J. Biol. Chem. 275*, 12763−12768.

5. Shen, Y., Romo, G. M., Dong, J. F., Schade, A., McIntire, L. V., Kenny, D., Whisstock, J. C., Berndt, M. C., Lopez, J. A., and Andrews, R. K. (2000) *Blood 95*, 903−910.
6. Cauwenberghs, N., Vanhoorelbeke, K., Vauterin, S., Westra, D. F., Romo, G., Huizinga, E. G., Lopez, J. A., Berndt, M. C., Harsfalvi, J., and Deckmyn, H. (2001) *Blood 98*, 652−660.
7. Nurden, A. T., and George, J. N. (2001) in *Hemostasis and Thrombosis. Basic Principles and Clinical Practice* (Colman, R. W., Hirsh, J., Marder, V. J., Clowes, E. W., and George, J. N., Eds.) 4th ed., pp 652−672, JB Lippincott, Philadelphia.
8. Hourdillé, P., Pico, M., Jandrot-Perrus, M., Lacaze, D., Lozano, M., and Nurden, A. T. (1990) *Br. J. Haematol. 76*, 521−530.
9. Simsek, S., Noris, P., Lozano, M., Pico, M., von dem Borne, A. E. G. Kr., Ribera, A., and Gallardo, D. (1994) *Br. J. Haematol. 88*, 839−844.
10. Lopez, J. A., Leung, B., Reynolds, C. C., Li, C. Q., and Fox, J. E. B. (1992) *J. Biol. Chem. 267*, 12851−12859.
11. Lopez, J. A., Weisman, S., Sanan, D. A., Sih, T., Chambers, M., and Li, C. Q. (1994) *J. Biol. Chem. 269*, 23716−23721.
12. Dong, J. F., Gao, S., and Lopez, J. A. (1998) *J. Biol. Chem. 273*, 31449−31454.
13. Sae-Tung, G., Dong, J. F., and Lopez, J. A. (1996) *Blood 87*, 1361−1367.
14. Budarf, M. L., Konkle, B. A., Ludlow, L. B., Michaud, D., Li, M., Yamashiro, D. J., McDonald-McGinn, D., Zackal, E. H., and Driscoll, D. A. (1995) *Hum. Mol. Genet. 4*, 763−766.
15. Kenny, D., Morateck, P. A., Gill, J. C., and Montgomery, R. R. (1999) *Blood 93*, 2968−2975.
16. Ludlow, L. B., Schick, B. P., Budarf, M. L., Driscoll, D. A., Zackai, E. H., Cohen, A., and Konkle, B. A. (1996) *J. Biol. Chem. 271*, 22076−22080.
17. Kunishima, S., Lopez, J. A., Kobayashi, S., Imai, N., Kamiya, T., Saito, H., and Naoe, T. (1997) *Blood 89*, 2404−2412.
18. Kunishima, S., Tomiyama, Y., Honda, S., Fukunishi, M., Hara, J., Inoue, C., Kamiya, T., and Saito, H. (2000) *Thromb. Haemostasis 84*, 112−117.
19. Moran, N., Morateck, P. A., Deering, A., Ryan, M., Montgomery, R. R., Fitzgerald, D. J., and Kenny, D. (2000) *Blood 96*, 532−539.
20. Nurden, P., and Nurden, A. (1996) *C. R. Acad. Sci. 319*, 717−726.
21. Hourdillé, P., Heilmann, E., Combrie, R., Winckler, J., Clemetson, K. J., and Nurden, A. T. (1990) *Blood 76*, 1503−1513.
22. Bihour, C., Durrieu-Jais, C., Macchi, L., Poujol, C., Coste, P., Besse, P., Nurden, P., and Nurden, A. T. (1999) *Arterioscler. Thromb. Vasc. Biol. 19*, 212−219.
23. Ruan, J., Schmugge, M., Clemetson, K., Cazes, E., Combrie, R., Bourre, F., and Nurden, A. T. (1999) *Br. J. Haematol. 105*, 523−531.
24. Pasquet, J. M., Noury, M., and Nurden, A. T. (2002) *Thromb. Haemostasis 88*, 115−122.
25. De la Salle, C., Baas, M. J., Lanza, F., Schwartz, A., Hanau, D., Chevalier, J., Gachet, C., Briquel, M. E., and Cazenave, J. P. (1995) *Br. J. Haematol. 89*, 386−396.
26. Ulsemer, P., Lanza, F., Baas, M. J., Schwartz, A., Ravanat, C., Briquet, M. E., Cranmer, S., Jackson, S., Cazenave, J. P., and De la Salle, C. (2000) *Thromb. Haemostasis 84*, 104−111.
27. Perrault, C., Moog, S., Rubinstein, E., Santer, M., Baas, M.-J., de la Salle, C., Ravanat, C., Dambach, J., Freund, M., Santoso, S., Cazenave, J.-P., and Lanza, F. (2001) *Thromb. Haemostasis 86*, 1238−1248.
28. Ulsemer, P., Strassel, C., Baas, M. J., Salamero, J., Chasserot-Golaz, S., Cazenave, J. P., De La Salle, C., and Lanza, F. (2001) *Biochem. J. 358*, 295−303.
29. Yagi, M., Edelboff, S., Disteche, C. M., and Roth, G. J. (1994) *J. Biol. Chem. 269*, 17424−17427.
30. Kobe, B., and Deisenhofer, J. (1994) *Trends Biochem. Sci. 19*, 415−421.
31. Meyer, S. C., and Fox, J. E. (1995) *J. Biol. Chem. 270*, 14693−14699.
32. Ramakrishnan, V., Reeves, P. S., DeGuzman, F., Deshpande, U., Ministri, K. M., and Phillips, D. R. (1999) *Proc. Natl. Acad. Sci. U.S.A. 96*, 13336−13341.
33. Kahn, M. L., Diacovo, T. G., Bainton, D. F., Lanza, F., Trejo, J., and Coughlin, S. R. (1999) *Blood 94*, 4112−4121.
34. Hillmann, A., Nurden, A., Nurden, P., Combrié, R., Claeyssens, S., Moran, N., and Kenny, D. (2002) *Thromb. Haemostasis 88*, 1026−1032.
35. Kobe, B., and Deisenhofer, L. (1995) *Nature 374*, 183−186.
36. Whisstock, J. C., Shen, Y., Lopez, J. A., Andrews, R. K., and Berndt, M. C. (2001) *Thromb. Haemostasis 87*, 329−333.
37. Kurokawa, Y., Ishida, F., Kamijo, T., Kunishima, S., Kenny, D., Kitano, K., and Koike, K. (2001) *Thromb. Haemostasis 86*, 1249−1256.
38. Poujol, C., Ware, J., Nieswandt, B., Nurden, A. T., and Nurden, P. (2002) *Exp. Hematol. 30*, 352−360.
39. Kieffer, N., Debili, N., Wicki, A., Titeux, M., Henri, A., Michel, Z., Breton-Gorius, J., Vainchenker, W., and Clemetson, K. J. (1986) *J. Biol. Chem. 261*, 15854−15862.
40. Gagnon, E., Duclos, S., Rondeau, C., Chevet, E., Cameron, P. H., Steele-Mortimer, O., Paiement, J., Bergeron, J. J., and Desjardins, M. (2002) *Cell 110*, 119−131.

BI026213D